0022-3565/10/3332-454–464$20.00
THE JOURNAL OF PHARMACOLOGY AND EXPERIMENTAL THERAPEUTICS
JPET 333:454–464, 2010

Vol. 333, No. 2
163337/3583341
Printed in U.S.A.

A Novel Sphingosine Kinase Inhibitor Induces Autophagy in Tumor Cells[S]

Vladimir Beljanski, Christian Knaak, and Charles D. Smith

Drug Discovery Core, Hollings Cancer Center (V.B., C.K., C.D.S.), and Department of Pharmaceutical and Biomedical Sciences (C.D.S.), Medical University of South Carolina, Charleston, South Carolina

Received November 3, 2009; accepted February 22, 2010

ABSTRACT

The sphingolipids ceramide, sphingosine, and sphingosine 1-phosphate (S1P) regulate cell signaling, proliferation, apoptosis, and autophagy. Sphingosine kinase-1 and -2 (SK1 and SK2) phosphorylate sphingosine to form S1P, shifting the balanced activity of these lipids toward cell proliferation. We have previously reported that pharmacological inhibition of SK activity delays tumor growth in vivo. The present studies demonstrate that the SK2-selective inhibitor 3-(4-chlorophenyl)-adamantane-1-carboxylic acid (pyridin-4-ylmethyl)amide (ABC294640) induces nonapoptotic cell death that is preceded by microtubule-associated protein light chain 3 cleavage, morphological changes in lysosomes, formation of autophagosomes, and increases in acidic vesicles in A-498 kidney carcinoma cells. ABC294640 caused similar autophagic responses in PC-3 prostate and MDA-MB-231 breast adenocarcinoma cells. Simultaneous exposure of A-498 cells to ABC294640 and 3-methyladenine, an inhibitor of autophagy, switched the mechanism of toxicity to apoptosis, but decreased the potency of the SK2 inhibitor, indicating that autophagy is a major mechanism for tumor cell killing by this compound. Induction of the unfolded protein response by the proteasome inhibitor *N*-(benzyloxycarbonyl)leucinylleucinylleucinal *Z*-Leu-Leu-Leu-al (MG-132) or the heat shock protein 90 inhibitor geldanamycin synergistically increased the cytotoxicity of ABC294640 in vitro. In severe combined immunodeficient mice bearing A-498 xenografts, daily administration of ABC294640 delayed tumor growth and elevated autophagy markers, but did not increase terminal deoxynucleotidyltransferase-mediated dUTP nick end labeling-positive cells in the tumors. These data suggest that ABC294640 promotes tumor cell autophagy, which ultimately results in nonapoptotic cell death and a delay of tumor growth in vivo. Consequently, ABC294640 may effectively complement anticancer drugs that induce tumor cell apoptosis.

Most current anticancer drugs kill actively dividing cells by the induction of apoptosis (Fulda, 2009). In addition to this "classical" cancer chemotherapy, approaches that block molecular pathways involved in tumor cell proliferation and therapies that induce alternative cell death pathways are of interest for drug development (Ricci and Zong, 2006). Apoptotic cell death involves a series of events leading to characteristic changes in cell morphology, including loss of cell membrane asymmetry, nuclear fragmentation, chromatin condensation, chromosomal DNA fragmentation, and activation of caspases (Ricci and Zong, 2006). Unfortunately, cancer cells often acquire resistance to agents that activate the apoptotic pathway (Fulda, 2009). Therefore, alternative cell death pathways are being examined for exploitation in cancer chemotherapy (Ricci and Zong, 2006).

Autophagy is a reversible catabolic adaptive process responsible for the degradation of long-lived proteins and cell survival during starvation and/or growth factor deprivation (Kundu and Thompson, 2008). During autophagy, parts of the cytoplasm are digested by lysosomes, thereby providing metabolites that are used for cell homeostasis. Although autophagy is a process with a major role in cell survival, it is

This work was supported by the National Institute of Healths [Grant R01-CA122226] (to C.D.S.). The Imaging Core of the Hollings Cancer Center is supported by National Institutes of Health [Grant CA138313-01] (to Dr. Andrew Kraft).

Article, publication date, and citation information can be found at http://jpet.aspetjournals.org.

doi:10.1124/jpet.109.163337.

[S] The online version of this article (available at http://jpet.aspetjournals.org) contains supplemental material.

ABBREVIATIONS: SK1, sphingosine kinase-1; SK2, sphingosine kinase-2; 3-MeA, 3-methyladenine; ABC294640, 3-(4-chlorophenyl)-adamantane-1-carboxylic acid (pyridin-4-ylmethyl)amide; DMS, dimethylsphingosine; LC3; tubulin-associated protein light chain 3; PI, propidium iodide; shRNA, short-hairpin RNA; SKI-2, 4-[[4-(4-chlorophenyl)-2-thiazolyl]amino]phenol; S1P, sphingosine 1-phosphate; SRB, sulforhodamine B; TUNEL, terminal deoxynucleotidyltransferase-mediated dUTP nick end labeling; MG-132, *N*-(benzyloxycarbonyl)leucinylleucinylleucinal *Z*-Leu-Leu-Leu-al; SCID, severe combined immunodeficient; mTOR, mammalian target of rapamycin; MEK, mitogen-activated protein kinase; ERK, extracellular signal-regulated kinase; PAGE, polyacrylamide gel electrophoresis; PBS, phosphate-buffered saline; PCR, polymerase chain reaction; MAPK, mitogen-activated protein kinase; PI3K, phosphatidylinositol 3-kinase; CI, combination index.

also capable of inducing cell death characterized by extensive digestion of intracellular organelles (Bursch et al., 2000). Importantly, a number of small molecules (including several anticancer drugs) activate autophagy both in vivo and in vitro in cancer cells (reviewed in Lefranc et al., 2007), indicating the importance of this biological process in the development of chemotherapeutics. Two potent sphingolipid second messengers, ceramide and sphingosine-1 phosphate (S1P), are also implicated in numerous cellular processes relevant to cell homeostasis, including apoptosis and autophagy (Cuvillier, 2007; Lavieu et al., 2008; Wymann and Schneiter, 2008). Conversion of proapoptotic sphingosine to prosurvival S1P is catalyzed by sphingosine kinase-1 (SK1) and SK2, and these enzymes are considered to be important targets for drug development (Delgado et al., 2006; Cuvillier, 2007). Overexpression of SK1 has been demonstrated in a number of solid tumors (French et al., 2003; Taha et al., 2004), where it may promote cell survival and drug resistance and regulate autophagy (Lavieu et al., 2006). In contrast to the role of SK1, much less is known about the roles of SK2 where its activities appear to be specific to cell type and cell conditions (reviewed in Taha et al., 2006).

Recently, we identified nonlipid, small-molecule inhibitors of SKs from a chemical library (French et al., 2003, 2006). Administration of these agents in a breast cancer allograft tumor model delays tumor growth without toxicity to mice (French et al., 2003, 2006). Our long-term goal is to identify specific small-molecule inhibitors of SK1 and SK2 and exploit pharmacological manipulation of SK enzymes for therapeutic benefits. Toward this end, we synthesized ABC294640 (Fig. 1A), as a first orally available, SK2-selective inhibitor. ABC294640 acts as a competitive inhibitor with respect to sphingosine with a K_i of 10 μM for recombinant human SK2 (French et al., 2010) and has therapeutic efficacy in models of diabetic retinopathy (Maines et al., 2006) and inflammatory bowel disease (Maines et al., 2008). Importantly, we have recently demonstrated that ABC294640 has favorable pharmacologic properties and can reach therapeutic levels in mouse plasma and tumors without overt toxicity (French et al., 2010).

The primary objective of the present studies was to determine the biological processes responsible for cancer cell death induced by ABC294640. Toward this goal, we used A-498 kidney, PC-3 prostate, and MDA-MB-231 breast tumor cells

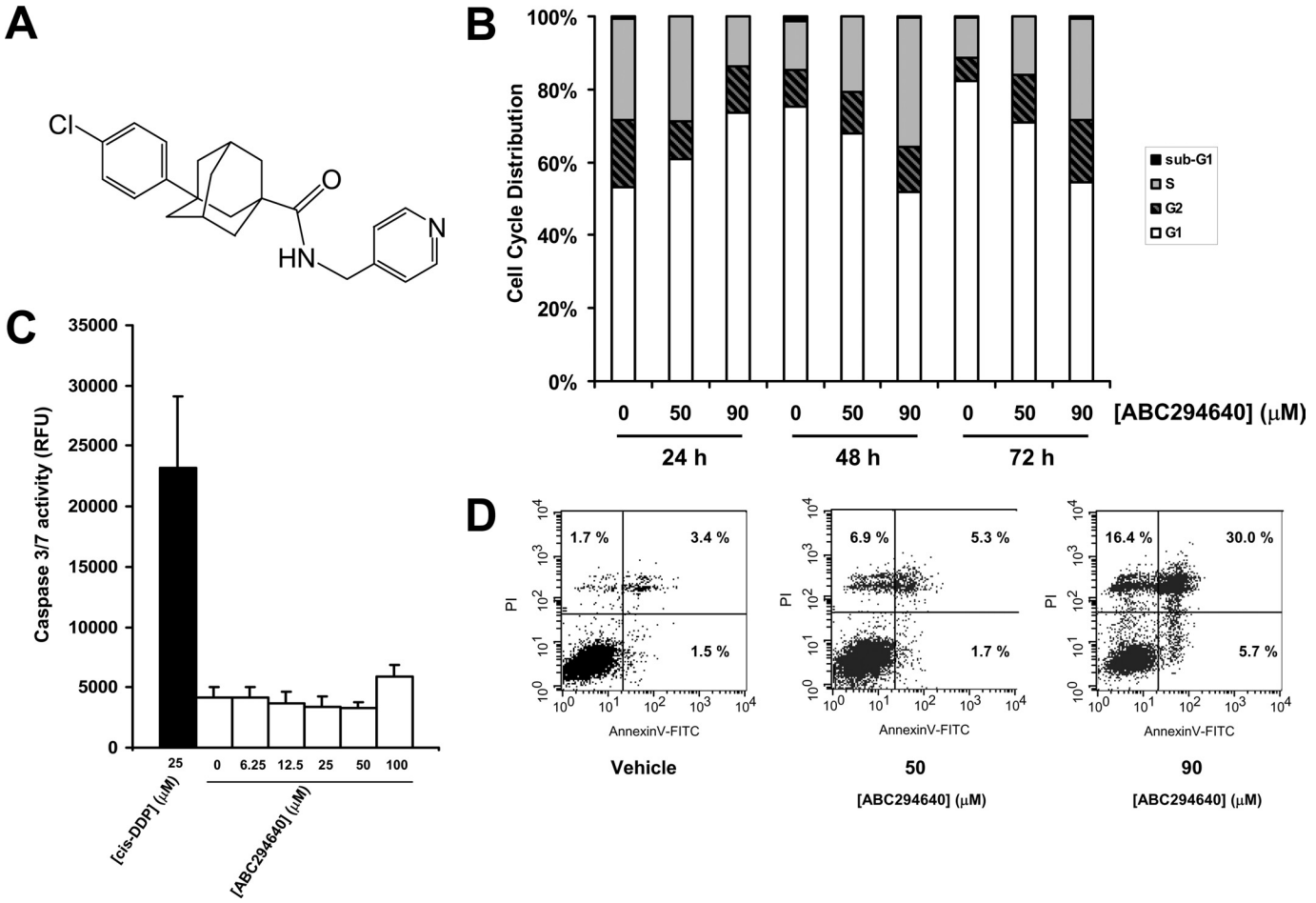

Fig. 1. ABC294640 induces nonapoptotic cell death in A-498 cells. A, chemical formula of ABC294640. B, cells were exposed to the indicated concentrations of ABC294640 and fixed at 24, 48 or 72 h. Nuclei were harvested and stained with PI, and the DNA content was analyzed by flow cytometry as described under *Materials and Methods*. C, cells were exposed to the indicated concentrations of ABC294640 for 72 h, and caspase 3/7 activity was measured by luminescence as described under *Materials and Methods*. Cisplatin (*cis*-DDP) was used as a control (black bar). Data represent mean ± standard error for three experiments. D, cells were exposed to the indicated concentrations of ABC294640 for 72 h and stained with PI and Annexin-V-FITC before analysis by flow cytometry as described under *Materials and Methods*. For each panel, the bottom left corner indicates Annexin V- and PI-negative cells; the bottom right corner indicates Annexin V-positive cells (apoptotic cells); the top-right corner indicates dead cells with membranes permeable to PI (PI-positive cells) stained with Annexin V; and the top left corner indicates dissociated nuclei. The percentage of total cells is indicated in each quadrant.

to show that ABC294640 induces nonapoptotic cell death preceded by markers of autophagy, including the acidification of cytoplasmic vesicles, increase in LC3 cleavage, and accumulation of autophagosomes. In addition, administration of ABC294640 to mice bearing A-498 xenografts led to a delay of tumor growth, and immunostaining of tumors from the treated mice revealed characteristics of the autophagic response in vivo.

Materials and Methods

Reagents and Cell Culture. Antibodies were purchased as follows: mTOR and phospho-mTOR (Ser2448), Akt, phospho-Akt, and p53 antibodies were from Cell Signaling Technology Inc. (Danvers, MA); ERK and phospho-ERK antibodies were from Santa Cruz Biotechnology Inc. (Santa Cruz, CA); LC3 antibody was from Novus Biologicals Inc. (Littleton, CO); pan-RAS antibody was from Oncogene Science (Cambridge, MA); and pan-Bcl-2 was from Sigma-Aldrich (St Louis, MO). CY3.5 conjugated to rabbit secondary antibody was purchased from Calbiochem (San Diego, CA), and all other antibodies were purchased from Abcam Inc. (Cambridge, MA). MitoTracker green, LysoTracker red, Annexin V, and Superscript III system were purchased from Invitrogen (Carlsbad, CA). ABC294640 was provided by Apogee Biotechnology Corporation (Hummelstown, PA). C6-ceramide and dimethylsphingosine (DMS) were purchased from Avanti Polar Lipids (Alabaster, AL). MG-132 was purchased from Calbiochem, and geldanamycin was a generous gift from Dr. Jennifer Isaacs (Medical University of South Carolina, Charleston, SC). All other chemicals were purchased from Sigma-Aldrich. shRNA lentiviral particles for SK2 and ATG7 were obtained from Santa Cruz Biotechnology Inc. A RNeasy kit was purchased from QIAGEN (Valencia, CA), and PerfeCTa SYBR Green Supermix for the iQ kit was purchased from Quanta Biosciences (Gaithersburg, MD). TUNEL staining kit and tetramethylrhodamine were purchased from Roche Diagnostics(Mannheim, Germany), and a Vectastain ABC kit was purchased from Vector Laboratories (Burlingame, CA). MDA-MB-231 mammary gland adenocarcinoma, PC-3 prostate adenocarcinoma, and A-498 kidney carcinoma cells were purchased from the American Type Culture Collection (Manassas, VA) and maintained in RPMI 1640 medium, Dulbecco's modified Eagle's medium, and Eagle's minimal essential medium, respectively, supplemented with 10% fetal bovine serum from Invitrogen (Carlsbad, CA). American Type Culture Collection performs quality control on the cell lines by testing short tandem repeat loci for all of our human cell lines. SCID mice were purchased from the National Cancer Institute (Bethesda, MD).

In Vitro Cell Treatment and Western Blot Analyses. To measure in vitro cell sensitivity to ABC294640 and other agents, standard sulforhodamine B (SRB) assays (Skehan et al., 1990) were performed as described previously (French et al., 2003).

For SDS-PAGE and immunoblotting, cells were plated at approximiately 10^6 cells/10 cm plate and treated with compounds as indicated under *Results*. Cells were lysed in buffer [50 mM Tris-HCl (pH 8), 1% sodium deoxycholate, 1% Nonidet P-40, 5 mM EDTA, 5 mM EGTA, and 150 mM NaCl], and the insoluble fraction was removed by centrifugation at 22,000*g* for 20 min. The soluble fractions were separated by SDS-PAGE on 10% gels, and proteins were electrophoretically transferred to a poly(vinylidene difluoride) membrane. Membranes were blocked with 10% bovine serum albumin and probed with various primary antibodies. All immunoblots were visualized by enhanced chemiluminescence and quantified by the ImageJ program (National Institutes of Health, Bethesda, MD).

Cell Cycle, Apoptosis, and Mitochondrial Membrane Integrity Analyses. For cell cycle analyses, cells were exposed to various concentrations of ABC294640 for 24, 48, or 72 h, washed twice with PBS, and incubated in 0.5 ml of PI staining solution (50 μg/ml propidium iodide, 40 μg/ml RNase A in PBS) for 30 min at 37°C. Cell cycle distributions were analyzed in the Medical University of South Carolina Flow Cytometry Facility with a Becton Dickinson FACSCalibur Analytical Flow Cytometer (BD Biosciences, San Jose, CA). The activities of caspases 3 and 7 were measured by the caspase-Glo 3/7 Assay (Promega, Madison, WI) according to the manufacturer's instructions. In brief, A-498 cells were grown in white 96-well plates at a density of 10,000 cells per well. After incubation with ABC294640, 100 μl of the caspase reagent was added and plates were incubated at room temperature for 30 min. After incubation, luminescence levels were determined by using a SpectraMax M5 plate reader (Invitrogen). Cells exposed to cisplatin were used as positive controls for apoptosis. For Annexin-V staining, after exposure to ABC294640, cells were trypsinized, resuspended in 10% fetal bovine serum-containing media, washed twice in PBS, and resuspended in Annexin binding buffer (10 mM HEPES, 140 mM NaCl, and 2.5 mM $CaCl_2$, pH 7.4). To 100 μl of the cell suspension, 5 μl of Annexin-V solution was added and the mixture was kept at room temperature for 15 min. After incubation, 400 μl of Annexin buffer was added and cells were immediately analyzed by flow cytometry. For the analysis of mitochondrial membrane function, cells exposed to ABC294640 or cisplatin (positive control) were stained with 100 nM tetramethyrhodamine for 30 min in growth medium, and after washing with PBS, cells were immediately analyzed by flow cytometry. Both adherent and floating cells were collected for the apoptosis and flow cytometry analyses.

Microscopy. Confocal images were obtained with a LSM 510 laser scanning confocal microscope (Carl Zeiss Inc., Thornwood, NY) in which the detector gain was equal in both experimental and control groups, except where indicated. Fields were randomly selected, and at least five different images with multiple cells were recorded per experimental condition. For electron microscopy, cells were grown in 25-mm flasks and exposed to 50 μM ABC294640 for 24 h. Cells were fixed with 2% cacodylate-buffered glutaraldehyde, postfixed with 2% osmium tetroxide, and dehydrated in ethanol. After dehydration, cells were infiltrated with a 1:1 solution of 100% EtOH and Embed 812, followed by embedding with pure Embed 812. Using a scroll saw, several representative areas were cut out and re-embedded for the correct orientation, after which 70-nm-thin sections were cut. Double staining was performed with uranyl acetate and lead citrate, and thin sections were examined with a JEOL (Tokyo, Japan) JEM 1010 transmission electron microscope.

Cell Organelle Staining. MitoTracker green was used to visualize mitochondria, and LysoTracker red was used to visualize lysosomes as described (Raval et al., 2006). Cells were plated overnight and exposed to various concentrations of ABC294640 for 24, 48, or 72 h at 37°C in 10% serum-containing Eagle's minimal essential medium (A-498), Dulbecco's modified Eagle's medium (PC-3), or RPMI 1604 medium (MDA-MB-231). Both LysoTracker red and MitoTracker green were added to achieve final concentrations of 50 nM. After 1 h of incubation, the medium was replaced with fresh media, and confocal imaging was performed. In some experiments, acidic vesicles were also stained with acridine orange (5 μg/ml), which was added to the prewarmed media containing 10% serum, and cells were incubated for 15 min. After replacement of the acridine orange-containing media with normal media, the cells were incubated for an additional 2 h before observation by confocal imaging. Immunofluorescent staining of LC3-II was performed on cells grown in eight-well chamber slides. After 24, 48 or 72 h exposure of cells to ABC294640, media were removed, and cells were fixed in 3.7% paraformaldehyde, permeabilized with 0.1% Triton X-100, blocked with 2% bovine serum albumin in Tris-buffered saline with Tween-20, and probed with 12 μg/ml LC3 antibody in blocking solution for 30 min. After removal of LC3 antibody and incubation in blocking solution for 60 min, cells were incubated with CY3.5-conjugated anti-rabbit secondary antibody at a concentration of 0.4 μg/ml. After 30 min at room temperature, cells were washed with Tris-buffered saline with Tween-20, mounted, and observed by confocal microscopy.

Xenograft Studies. Animal studies have been carried out in accordance with the Guide for the Care and Use of Laboratory Animals by the U.S. National Institutes of Health. SCID mice (6–8 weeks old) were injected with 3×10^6 A-498 cells per mouse, and after 3 to 4 weeks, mice bearing tumors of 100 to 150 mg were treated with either vehicle or 50 mg/kg ABC294640 5 days/week for 4 weeks (eight mice per cohort). Tumors were measured twice per week, and volumes were calculated by using the following formula: volume = $1/2 \times \text{length} \times \text{width}^2$. At the end of the treatment, four animals from each cohort were sacrificed, and the paraffin-embedded tumor sections were stained with hematoxylin/eosin. Additional sections were deparaffinized and rehydrated in graded alcohols using standard procedures, and then subjected to TUNEL according to the manufacturer's instructions. The percentage of TUNEL-positive cells was determined by counting at least 100 cells each from at least three randomly selected fields. Additional sections were blocked with 10% normal goat serum in a humid chamber for 30 min, and then incubated antibodies for beclin 1 or LC3 overnight at 4°C, followed by secondary antibody for 60 min at room temperature.

shRNA Knockdown and Reverse Transcription–Polymerase Chain Reaction Analyses of Clones. For shRNA knockdown of Atg7 or SK2, A-498 cells were plated at approximately 25% confluence and incubated 24 h later with the appropriate viral particles in the presence of 5 μg/ml Polybrene. After 24 h, cells were split 1:5 and selected by the addition of puromycin at 4 μg/ml. After the isolation of puromycin-resistant colonies, cells at approximately 75% confluence were harvested for analysis while still under selection. Total RNA was isolated and converted to cDNA, and the expression of the SK2 gene relative to 18S was assessed by real-time PCR using a Bio-Rad (Hercules, CA) MyiQ iCycler instrument. Forward primers were 5′-GGAGGAAGCTGTGAAGATGC-3′ (SK2) and 5′-TTGGAGGGCAAGTCTGGTG-3′ (18S), and the reverse primers were 5′-GCAACAGTGAGCAGTTGAGC-3′ (SK2) and 5′-CCGCTCCCAAGATCCAACTA-3′ (18S). Relative levels of SK2 were calculated as described previously (Edwards et al., 2000).

Statistical Analyses. Two-way analysis of variance was used to access the significance of differences between experimental groups. Both unpaired *t* test and Welch's corrected *t* test were performed to access statistical significance. Differences were considered to be significant for $P < 0.05$. The nature of the interaction between ABC294640 and MG-132 or geldanamycine was calculated by using the Chou-Talalay method for determining the combination index (Chou and Talalay, 1984) using CalcuSyn software (Biosoft, Ferguson, MO). Based on this approach, combination index values <0.9 are considered synergistic, values >1.1 are antagonistic, and values 0.9 to 1.1 are considered to be additive.

Results

To characterize the potential effects of ABC294640 on apoptosis, nuclei from control and treated cells were stained with PI and analyzed by flow cytometry (Fig. 1B). The results show that only a small fraction of ABC294640-treated cells (<1%) contained sub-G_1 amounts of DNA, even at toxic drug concentrations (>50 μM) and long treatment times (72 h). The absence of DNA fragmentation is an indication that ABC294640 does not induce apoptosis in A-498 cells. These results were corroborated by the lack of caspases 3/7 activation in ABC294640-treated cells even after 72 h of exposure (Fig. 1C). Annexin-V quantification of apoptosis/necrosis is based on the asymmetric distribution of phosphatidylserine, which, upon induction of apoptosis, flips from the cytoplasmic face of the plasma membrane to the outer leaflet where it becomes available to bind with Annexin-V. Addition of PI differentiates necrotic or late apoptotic cells from early apoptotic cells. As demonstrated in Fig. 1D, Annexin-V staining of ABC294640-treated cells at a toxic concentrations (50 or 90 μM) and long exposure time (72 h) revealed an increase in the population of cells that were stained by Annexin-V + PI or PI alone (30 and 16.4%, respectively), but only a few apoptotic cells were stained by Annexin-V but not PI (< 6% at 90 μM). This is consistent with the cells becoming permeable to PI (because of compromise of plasma membrane) without previous activation of the apoptotic machinery. The data from all three apoptosis assays indicate that the majority of A-498 cells exposed to ABC294640 die without displaying the specific features of apoptosis.

The lack of apoptotic indicators in ABC294640-treated A-498 cells prompted us to investigate other processes that can lead to cell death. Recent reports indicate roles for autophagy and lysosomes in tumor cell death induced by certain cancer chemotherapeutics (Lefranc et al., 2007; Klionsky et al., 2008), so various autophagy markers were examined. Tubulin-associated protein LC3 is a cytosolic protein that is cleaved upon the induction of autophagy, yielding cytosolic LC3-I (18 kDa) and autophagosome-associated LC3-II (16 kDa). We found that ABC294640 caused dose- and time-dependent cleavage of LC3 in A-498 cells, which progressively increased over the 72-h time course (Fig. 2A). The known autophagy-inducing sphingolipid ceramide also promoted the rapid and pronounced cleavage of LC3. The dual SK1 and SK2 inhibitors 4-[[4-(4-chlorophenyl)-2-thiazolyl]amino]phenol (SKI-2) and DMS also induced LC3 cleavage at 24, 48, or 72 h (Fig. 2B). Confocal fluorescence microscopy of cells exposed to any of the three SK inhibitors revealed the existence of punctate dots in the cytoplasm, indicating recruitment of LC3-II to autophagosomes (Fig. 2C). Quantification of LC3-positive A-498 cells exposed to ABC294640, SKI-2, or DMS revealed a statistically significant increases in LC3-positive cells (Fig. 2D). Although DMS is known to alter the activities of other kinases (Igarashi et al., 1989; Megidish et al., 1995), the demonstration that LC3 cleavage and the formation of autophagosomes is induced by three structurally distinct SK inhibitors supports the hypothesis that autophagy is a common response to the pharmacological inhibition of SK rather than a specific effect of ABC294640.

Electron microscopy was performed to further confirm the induction of autophagy in A-498 cells. Exposure of the cells to 50 μM ABC294640 for 24 h resulted in the production of many large empty vacuoles and autophagic vacuoles containing residual digested material or intact organelles (Fig. 3A). Consistent with the previous data, no chromatin condensation or nuclear fragmentation (signs of apoptotic death) was observed. In contrast, only a few small autophagic vacuoles were observed in the vehicle-treated cells (Fig. 3B).

Autophagy often serves as a defense mechanism to various toxic insults (Jin and White, 2008). To establish whether autophagy is a defense mechanism in A-498 cells, we attempted to eliminate autophagy by creating a stable shRNA knockdown of the Atg7 gene (Yu et al., 2004). However, this resulted in lethality such that no stable clones could be established, suggesting the importance of autophagy in the survival of these tumor cells. Therefore, we pharmacologically blocked autophagy with an inhibitor of class III phosphatidylinositol 3-kinases (PI3Ks), 3-methyladenine (3-MeA) as described previously (Herman-Antosiewicz et al., 2006; Cui et al., 2007). A-498 cells were exposed to ABC294640

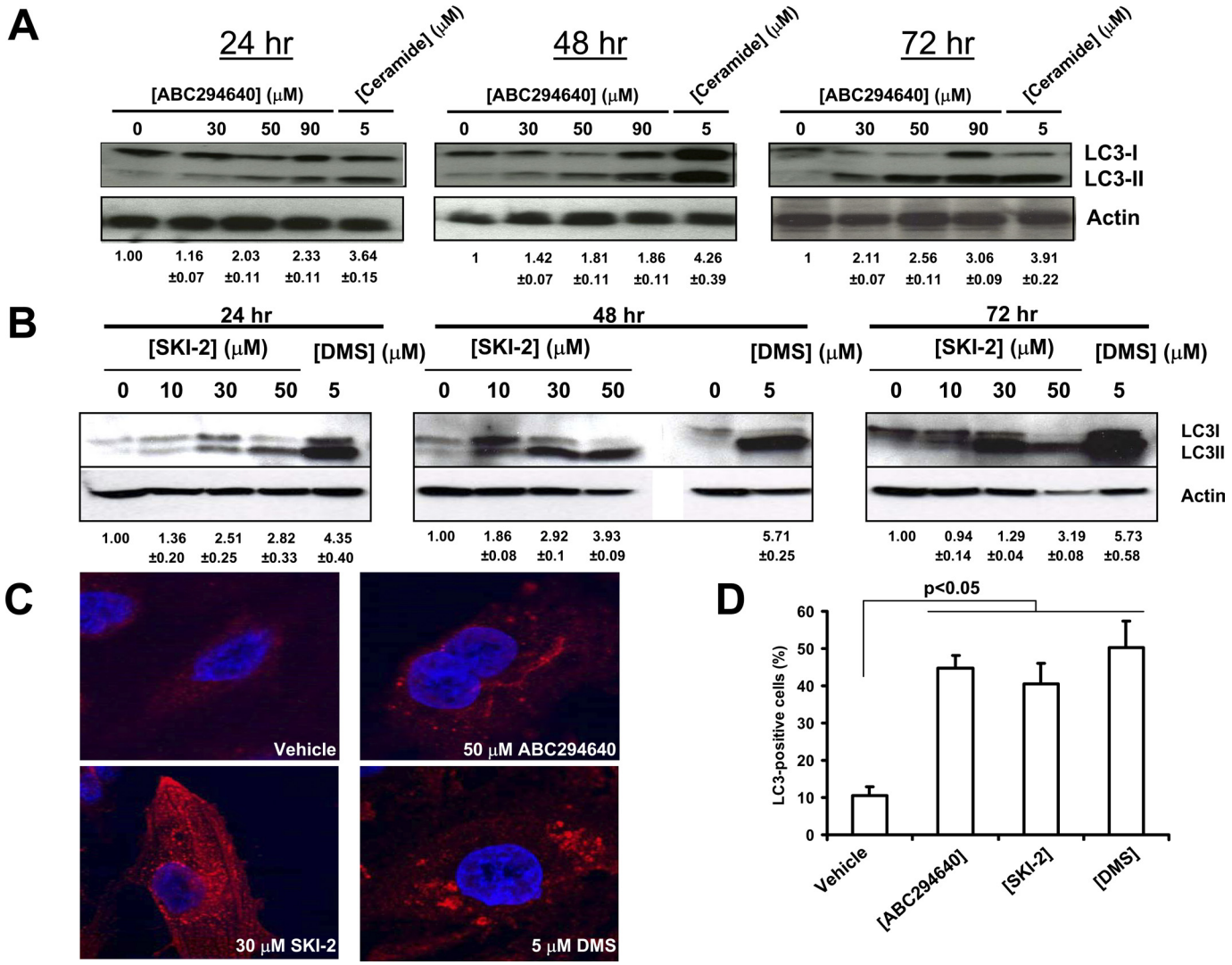

Fig. 2. Effects of SK inhibitors on LC3 cleavage and formation of autophagosomes in A-498 cells. A, cells were treated with the indicated concentrations of ABC294640 or 5 μM ceramide for the indicated times. The generation of LC3-II was then examined by Western blotting as described under *Materials and Methods*. Equal loading was confirmed by stripping and reprobing with anti-actin antibody. B, cells were exposed to the indicated concentrations of SKI-2 or 5 μM DMS, and the LC3 cleavage was assessed by Western blotting of cell lysates at 24, 48 or 72 h as described under *Materials and Methods*. C, A-498 cells were exposed to the vehicle, ABC294640, SKI-2, or DMS for 48 h, and then fixed and immunostained for LC3 as described under *Materials and Methods*. D, quantification of LC3-positive cells. Cells were exposed to 50 μM ABC294640, 30 μM SKI-2, or 5 μM DMS for 48 h. Data represent mean ± S.E. for three experiments. The numbers below the Western blots indicate the relative LC3-II/actin ratios compared with the vehicle-treated cells ± S.E.

alone or in the presence of 5 mM 3-MeA, and the DNA content, caspase 3/7 activity, and cell survival were measured. Consistent with the results described above, neither ABC294640 alone nor 3-MeA alone induced DNA fragmentation (Fig. 3C). However, treatment with the ABC294640 plus 3-MeA combination resulted in significant accumulations of cells with fragmented DNA. In addition, cells treated with the combination expressed substantial caspase 3/7 activity indicative of apoptosis, whereas neither compound alone caused this effect (Fig. 3D). Addition of 3-MeA to the cultures reduced the cytotoxicity of ABC294640 and DMS (Fig. 3E), suggesting that autophagy is at least in part responsible for cell death. Addition of 3-MeA to A-498 cells blocked the production of LC3-II in response to ABC294640 (Supplemental Fig. 1A), demonstrating the 3-MeA was effective in suppressing autophagy in these cells. These results were further supported by combining ABC294640 with the autophagy inhibitor chloroquine (Amaravadi et al., 2007), which resulted in antagonistic cytotoxicity for the two compounds (data not shown).

To further examine the potential role of SK2 in the induction of autophagy, we created stable SK2 knockdown clones from A-498 cells using shRNA delivered by lentivirus. In contrast with the studies with Atg7, several clones were established. However, examination of the levels of SK2 mRNA expression in these clones by quantitative real-time PCR indicated that SK2 knockdown was variable and incomplete (Supplemental Fig. 1B), such that no clones with SK2 mRNA levels below approximately 30% of control cells were obtained. This is consistent with our studies using siRNA directed against SK2 that show that suppression of SK2 blocks A-498 cell proliferation (unpublished data). The partial SK2-knockdown clones did not have substantial increases in the levels of LC3-II (Supplemental Fig. 1C), sug-

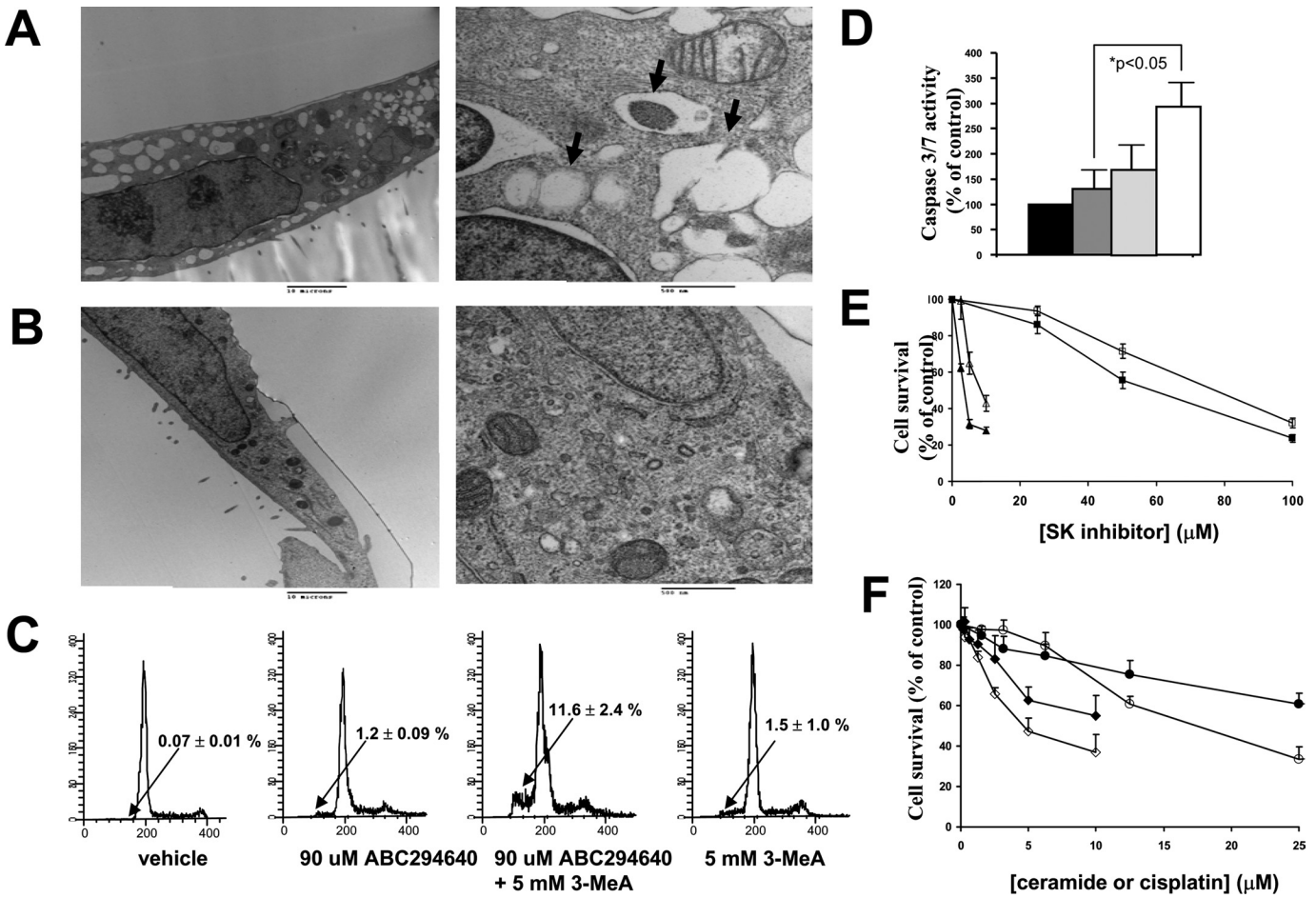

Fig. 3. Induction of autophagic vacuolization or apoptosis by ABC294640 in A-498 cells. A and B, cells were treated with 50 μM ABC294640 (A) or vehicle (B) for 24 h, and electron micrographs were generated as described under *Materials and Methods*. Representative micrographs at low magnification (left, bar = 10 μm) or high magnification (right, bar = 0.5 μm) depicting the ultrastructure of the cells are shown. Arrows indicate autophagic vacuoles. C and D, A-498 cells were treated with ABC294640 or 3-MeA alone or in combination for 72 h, and then processed for analyses of their DNA content (C) or caspase 3/7 activity (D) as described under *Materials and Methods*. The black bar represents caspase 3/7 activity in cells treated with the vehicle, the dark gray bar represents caspase 3/7 activity in cells treated with 90 μM ABC294640, the light gray bar represents caspase 3/7 activity in cells treated with 5 mM 3-MeA, and the white bar represents caspase 3/7 activity in cells treated with both after 72 h. E, A-498 cells were treated with either ABC294640 (squares) or DMS (triangles) alone (filled symbols) or in combination with 5 mM 3-MeA (open symbols) for 48 h, and cell survival was assessed by SRB staining. F, A-498 wild-type cells (filled symbols) or SK2 shRNA-transfected A-498 cells (open symbols) were treated with cisplatin (circles) or ceramide (squares) for 48 h, and their survival was assessed by the standard SRB assay.

gesting that partial knockdown of SK2 does not induce autophagy. However, partial knockdown of SK2 enzyme sensitized the A-498 cells to both apoptosis- and autophagy-inducing agents represented by cisplatin and ceramide, respectively (Fig. 3F), suggesting that the combination of ABC294640 with other chemotherapeutics may be therapeutically effective.

Because basic lipophilic compounds can act as lysosomotropic agents and are thus possible autophagy modulators, lysosomal morphology was assessed to gain further insight into the mechanisms by which ABC294640 induces autophagy. Compared with control cells, treatment with ABC294640 for 24 h resulted in enhanced accumulation of LysoTracker Red dye and increases in the size of lysosomes ("swelling") (Supplemental Fig. 2). When quantified, the average pixel intensity for lysosomes in ABC294640-treated cells was 204, compared with 160 for vehicle-treated cells ($p < 0.05$ for the two values), indicating higher lysosomal accumulation of the dye in ABC294640-treated cells. Increased acidification of cytoplasmic organelles was confirmed by acridine orange staining. Acridine orange enters cellular acidic compartments and becomes protonated and sequestered. At low pH, the dye emits red-orange light when exited by blue light. Staining of ABC294640-treated cells with acridine orange revealed increases in both the number and size of acidic vesicular organelles (Supplemental Fig. 2). For comparison, we exposed cells to ceramide or tamoxifen, two molecules known to induce autophagy in cancer cells (Scarlatti et al., 2004; Pattingre et al., 2008). As indicated by staining with LysoTracker or acridine orange, A-498 cells exposed to either tamoxifen or C6-ceramide displayed similar lysosomal swelling, confirming that both tamoxifen and ceramide are lysosomotropic agents (Supplemental Fig. 2, D and E). Staining of mitochondria with MitoTracker green revealed that ABC294640-treated cells accumulated normal amounts of the MitoTracker dye, indicating that mitochondria of those cells remains polarized during drug treatment (Poot et al., 1996). This was confirmed by staining with tetramethylrhodamine, a cell-permeable fluorescent dye that is readily sequestered by active mitochondria and detected by flow cytometry, because ABC294640 did not impair dye accumulation (data not shown).

To assess the generality of the effects of ABC294640 on autophagy, two additional cancer cell lines, prostate (PC-3) and breast (MDA-MB-231) adenocarcinoma cells, were used. Exposure of those cells to ABC294640 also resulted in cell death that was not associated with DNA fragmentation, even at high concentrations (90 μM) and long exposure times (72 h) (Fig. 4). However, in both MDA-MB-231 and PC-3 cells, ABC294640 caused the dose-dependent cleavage of LC3 at 24 h and increases in acidic compartments in the cytosol. Therefore, induction of autophagy by ABC294640 is not limited to a specific cell line, but rather appears to be a common response among tumor cells.

We also measured the levels of several signaling and survival proteins in A-498 cells exposed to ABC294640 by immunoblotting. The expression levels of beclin 1, which is a tumor suppressor and one of the key proteins in autophagy pathway, was progressively increased at 48 and 72 h with increases in ABC294640 concentration (Fig. 5A). Involvement of the MEK/ERK pathway in the antitumor activity of ABC294640 was demonstrated by decreased levels of phospho-Akt and phospho-ERK in the A-498 cells treated with this compound. Interestingly, even though the Akt and ERK pathways can activate mTOR signaling, which blocks autophagy (Meijer and Codogno, 2006), ABC294640 did not significantly decrease phospho-mTOR levels. Therefore, autophagy in A-498 cells induced by treatment with ABC294640 does not result from changes in the phosphorylation status of mTOR, but is associated with upregulation of beclin 1.

Anticancer chemotherapy is usually administered as a combination of different drugs by specific schedules. Based on the discovery of autophagic cell death induced by ABC294640, and knowing that some misfolded proteins are degraded by autophagy (Ding and Yin, 2008), we hypothesized that drugs that induce the unfolded protein response, such as proteasome inhibitors (e.g., MG-132) or heat shock protein 90 inhibitors (e.g., geldanamycin), could affect the cytotoxicity of ABC294640. Therefore, A-498 cells were exposed to ABC294640 plus geldanamycin or MG-132 combinations at various drug–drug ratios. The surviving fraction of the cell population was determined at 72 h of drug treatment (Fig. 5, B and C). Analyses of the combination indexes (CalcuSyn) confirmed that combinations of ABC294640 and geldanamycin are synergistically cytotoxic, i.e., with combination indexes <1.0 (Fig. 5B). Similarly, combinations of ABC294640 and MG-132 were also synergistically toxic (Fig. 5C).

To further study the in vivo antitumor properties of ABC294640, we used SCID-bearing xenografts of A-498 cells. As shown in Fig. 6A, daily administration of 50 mg/kg ABC294640 led to a statistically significant delay in tumor growth over the 4 weeks of treatment. After 28 days, tumor tissues were excised, fixed, and sectioned, and slides were immunostained to assess the levels of beclin 1 and LC3 and stained by TUNEL to establish the number of apoptotic cells (Fig. 6B). As shown in Fig. 6C, the intensity of staining of both beclin 1 and LC3 was increased in the tumors from mice that were exposed to ABC294640 compared with the vehicle-treated mice. In contrast, no differences in the number of apoptotic cells were observed in ABC494640- and vehicle-treated tumors (Fig. 6, B and C, bottom), indicating that an increase in apoptosis is not responsible for the delay of tumor growth in vivo in this model. These data are consistent with

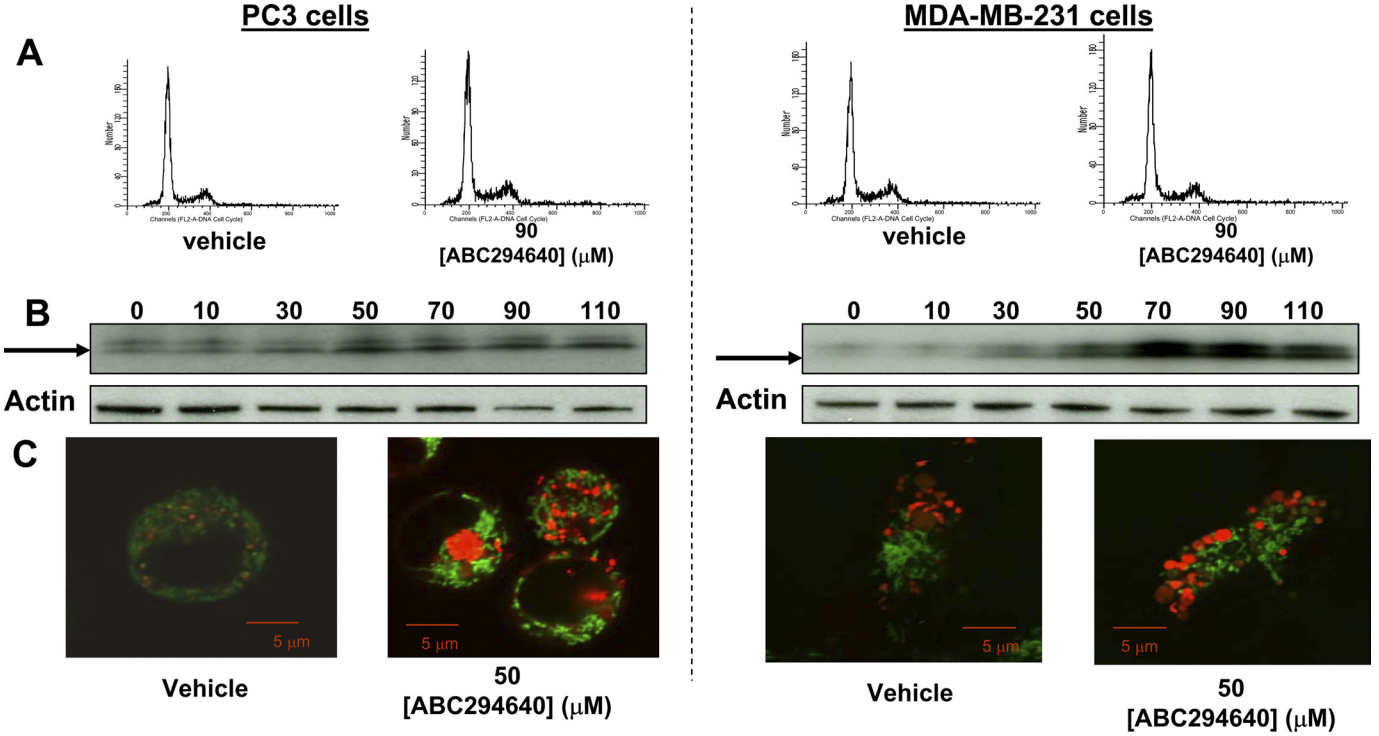

Fig. 4. Activation of autophagy in PC-3 and MDA-MB-231 cells. A, PC3 cells (left) or MDA-MB-231 cells (right) were treated with vehicle or 90 μM ABC294640 for 72 h. The cells were then fixed in ethanol and stained with PI and analyzed by flow cytometry as described under *Materials and Methods*. B, PC3 (left) or MDA-MB-231 (right) cells were exposed to the indicated concentrations of ABC294640 (μM) for 24 h before lysis and immunoblotting. The arrow indicates LC3-II. C, PC3 (left) or MDA-MB-231 (right) cells were exposed to 50 μM ABC294640 for 24 h and stained with MitoTracker green and LysoTracker red dyes, and confocal imaging was performed as described under *Materials and Methods*.

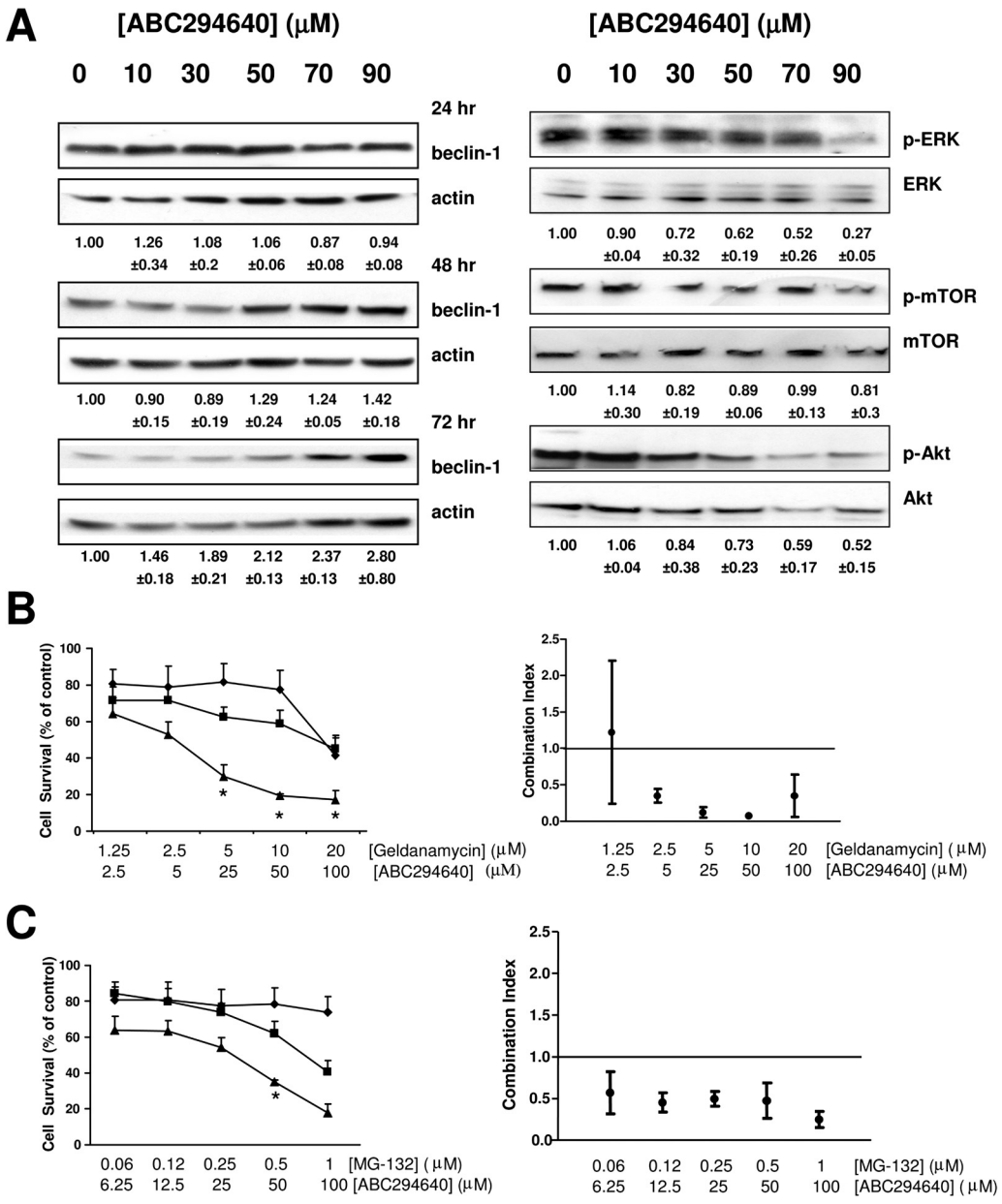

Fig. 5. Effects of ABC294640 on signaling pathways and combination effects of ABC294640 with geldanamycin or MG-132. A, cells were exposed to the indicated concentrations of ABC294640 for 48 h, fractionated by SDS-PAGE, and probed for the indicated proteins by Western blotting as described under *Materials and Methods*. Beclin 1 expression at 24 and 72 h is also shown. The numbers below the Western blots indicate either the relative phosphorylated protein/total protein ratios compared with the vehicle-treated cells ± standard error or the relative beclin-1/actin ratios compared with the vehicle-treated cells ± standard error. B and C, A-498 cells were exposed to the indicated concentrations of ABC294640 alone (gray bars), geldanamycin (B, white bars), MG-132 (C, white bars), or combinations of ABC294640 and geldanamycin or MG-132 (black bars), and survival was assessed by the SRB assay at 72 h. Combination indexes (CI) calculated by CalcuSyn for the respective combinations are shown on the right. CI values between 0 and 1 indicate synergism, and CI values above 1 indicate antagonism. Strong synergism is indicated by values close to 0. *, $p < 0.05$.

the induction of autophagy and nonapoptotic cell death observed in vitro.

Discussion

The well established involvement of S1P in cell growth and tumor development prompted us to develop several small-molecule SK inhibitors with in vitro and in vivo activity (French et al., 2003, 2006; Maines et al., 2006, 2008; Smith et al., 2008). A current lead SK2 inhibitor, ABC294640, was developed to improve the oral bioavailability and enzyme specificity that hampered the development of other lipid-mimetic SK inhibitors (French et al., 2010). We have shown previously that ABC294640 has anti-inflammatory activity in vivo (Maines et al., 2006, 2008; Smith et al., 2008) and in this work that it also has antitumor activity (Fig. 6). Pharmacokinetic studies of ABC294640 indicate that the compound reaches a peak plasma concentration of approximately 20 μM after an oral dose of 50 mg/kg and is eliminated with a half-time of clearance of approximately 4.5 h (French et al., 2010), suggesting that even more pronounced antitumor effects can be obtained with higher doses and/or more frequent administration. ABC294640 is currently in certified Good Laboratory Practice toxicology studies and is expected to enter clinical trials in 2010. The work presented here is the first detailed study of the antitumor properties of ABC294640 in human cancer cells both in vitro and in vivo. Unexpectedly, we found that exposure of tumor cells to this agent induces autophagy that preceded, and likely led to, the nonapoptotic cell death.

The exact mechanism by which autophagy kills cancer cells has not been established. However, it is likely that prolonged activation of autophagic degradation of cellular components, e.g., key proteins and organelles responsible for cell metabolism and (possibly) apoptosis, ultimately push the cells beyond the point of recovery and into nonapoptotic death (Fig. 7). This is similar to the proposed mechanism of

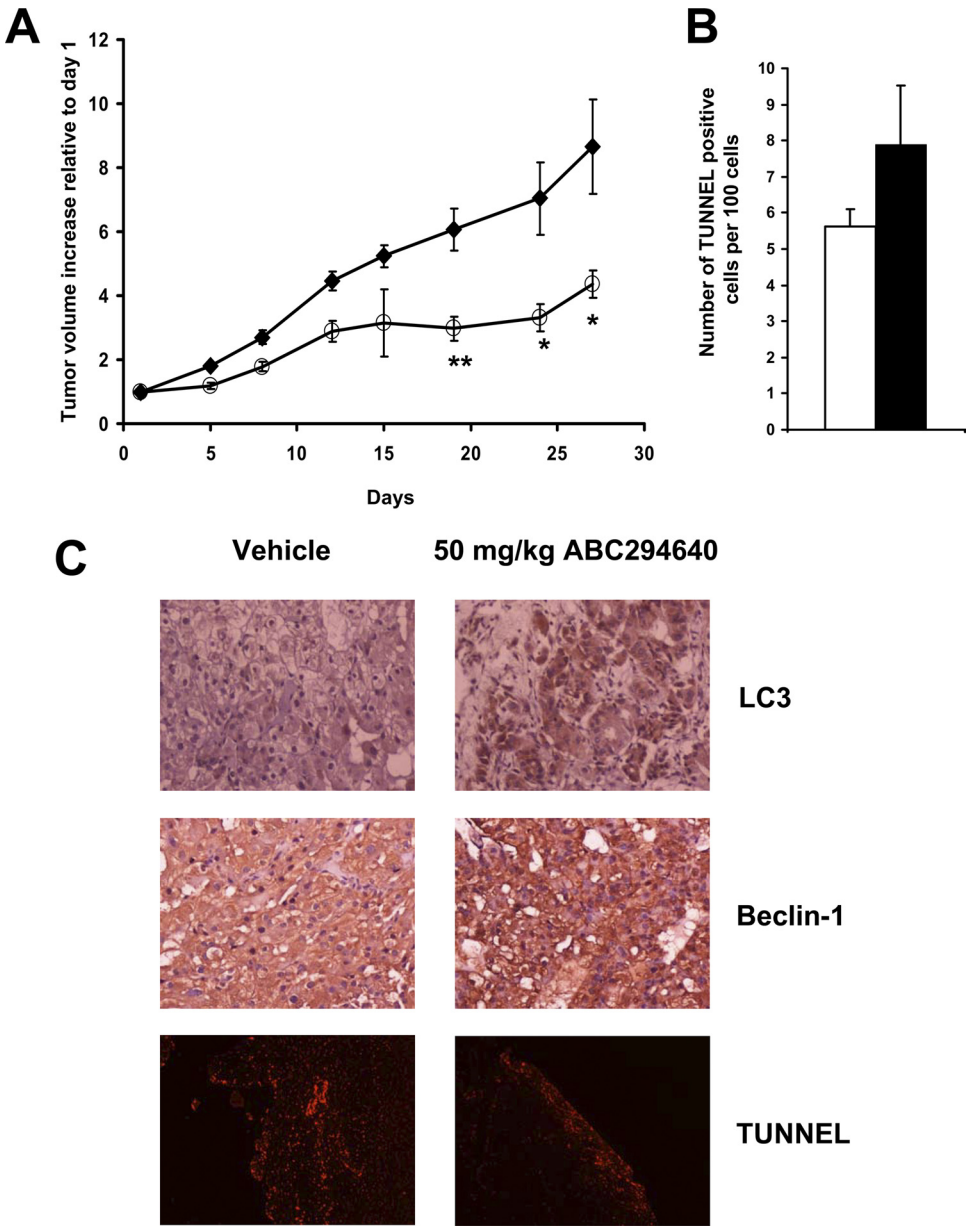

Fig. 6. Effects of ABC294640 on tumor growth in mice and histological characterization of ABC294640-treated tumors. A, female SCID mice (n = 8 per group) were injected subcutaneously with A-498 cells suspended in PBS. After palpable tumors were formed, the animals were treated every day by oral gavage with 0 (♦) or 50 mg/kg ABC294640 (○). Values represent the mean ± S.E. tumor volume normalized to treatment day 1 for each mouse. *, $p < 0.05$; **, $p < 0.01$. Mice were sacrificed on day 27 after the beginning of treatment, and tumors were fixed in formalin and sections from tumors were stained for TUNEL and immunostained for LC3 and beclin 1 as described under *Materials and Methods*. B, quantification of TUNEL-positive cells. The black bar represents vehicle-treated tumors, and the white bar represents ABC294640-treated tumors. Data represent mean ± S.E. for three experiments. C, histologic characterization of ABC294640-treated tumors.

action of proteasome inhibitory anticancer drugs such as Velcade. In A-498 cells exposed to ABC294640, we observed down-regulation of the prosurvival MAPK pathway in parallel with down-regulation of the antiapoptotic Akt pathway, in spite of cells being maintained in complete medium. However, only a small population of cells was able to activate the apoptotic pathway, unless autophagy was blocked by the addition of 3-MeA. Therefore, autophagy appears to be the dominant mechanism for cell death in ABC294640-treated tumor cells.

Factors that control tumor cell fate include receptors, enzymes (such as SK1/2), and transcription factors, all of which are connected into complex and often redundant signaling networks. A current approach in clinical oncology is to use combinations of multiple drugs to circumvent this redundancy. One of the major drawbacks in this approach is the need to use multiple dugs simultaneously, which can result in cumulative toxicity (Hu and Xuan, 2008). An effective way to overcome this obstacle is to activate alternative processes that can lead to tumor cell death. Apoptosis has received the most attention in studies of tumor cell death, but there are clearly alternate mechanisms by which cancer cells can be removed. One understudied pathway is autophagy, an evolutionarily conserved process that allows cells to survive during the stress of nutrient deprivation. During autophagy, parts of the cytoplasm and organelles are engulfed in double-membrane vesicular structures known as autophagosomes. These vesicles then fuse with lysosomes and their contents are degraded by lysosomal hydrolases. There is a growing body of evidence indicating that autophagy is activated upon treatment with some anticancer drugs, but its contribution to cell death and/or anticancer drug resistance remains unclear (Lefranc et al., 2007; Wang et al., 2008). Recently, a small molecule that selectively targets von Hippel-Lindau tumor suppressor gene-deficient renal cell carcinoma was shown to kill tumor cells exclusively through activation of autophagy, demonstrating that this mechanism can lead to tumor cell death (Turcotte et al., 2008). Interplay between apoptosis

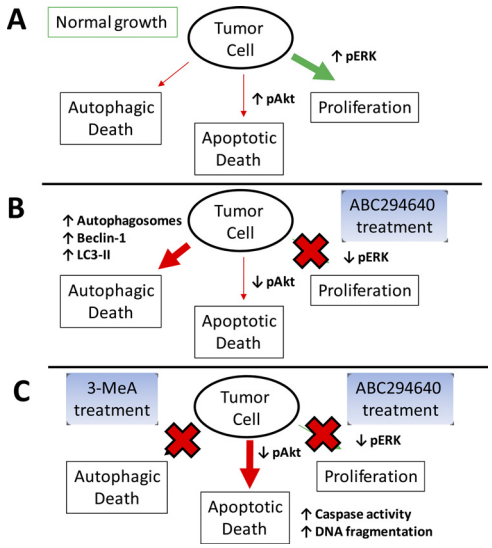

Fig. 7. A model for tumor cell death in response to ABC294640. A, under normal growth conditions, the MAPK and Akt pathways are active, resulting in high cell proliferation and low apoptosis. There is a basal level of autophagy to provide metabolites to support the rapid proliferation and energy demand of the cells. B, upon exposure to ABC294640, MAPK and Akt pathways are down-regulated, thereby inhibiting proliferation and attenuating the restriction on apoptosis. Concurrently, ABC294640-induced production of ceramide (via inhibition of SK) accelerates autophagy (manifested as increased production of autophagosomes) to an unsustainable point, resulting in autophagic death. C, in the presence of 3-MeA, autophagy is blocked, which drives the tumor cells into apoptosis, indicated by DNA fragmentation and caspase activation.

and autophagy occurs, because blocking of autophagy often promotes apoptosis (Thorburn, 2008).

Initiation of autophagy and the elongation of autophagosomes involve the actions of several proteins, including the scaffold protein beclin 1 and the lipidated form of LC3-II, which associates with autophagosomes. Several signaling proteins modulate this process. For example, the mTOR signaling network receives input from growth factor receptors via the class I PI3K signaling pathway. Both the PI3K/Akt/mTOR and MEK/ERK pathways suppress autophagy when activated. In A-498 cells, upon treatment with ABC294640, we observed decreases in levels of phospho-Akt and phospho-ERK1/2, but no change in phosphorylation status of mTOR, an indication that autophagy induced by ABC294640 does not require decreased levels of phospho-mTOR. In contrast to reports in other systems (Cheng et al., 2007), we found no changes in the levels of the autophagy (and apoptosis) inhibitor Bcl-2 (data not shown), which binds to and inhibits beclin 1. On the other hand, up-regulation of beclin 1 protein levels in A-498 cells exposed to ABC294640 was observed at 72 h. A similar up-regulation of beclin 1 was observed in human colon cancer HT-29 cells undergoing autophagy upon exposure to C6-ceramide (Scarlatti et al., 2004). We hypothesize that up-regulation of beclin 1 is required for the long duration of autophagy induced by ABC294640. In translation to an animal model, daily administration of ABC294640 led to a delay in the growth of subcutaneous xenografts of kidney carcinoma cells. Up-regulation of beclin 1 and LC3, and a lack of apoptosis (measured by TUNEL assay), was also found by immunostaining of the tumor tissues. These results may indicate that the induction of autophagy rather than an increase in apoptosis in vivo plays a major role in the delay in tumor growth.

A-498 kidney carcinoma cells were chosen as the primary model for biochemical and cellular studies because kidneys have relatively high expression of SK2 enzyme (Taha et al., 2006). In addition, renal cancer is particularly difficult to treat clinically. Therefore, it is important to understand which death mechanisms in these cells can be activated by SK inhibitors to facilitate their further development as potential kidney cancer drugs. This study also represents the first report of autophagy in kidney carcinoma cells. Importantly, the mechanistic findings extend to other cancer cell lines, because exposure of MDA-MB-231 and PC-3 cells to ABC294640 does not activate apoptosis, but rather leads to the cleavage of the LC3 protein and acidification of intracellular compartments, suggesting its general ability to promote tumor cell autophagy. Furthermore, we observed LC3 cleavage and formation of autophagosomes in A-498 cells exposed to other structurally divergent SK inhibitors (DMS and SKI-2), indicating that other SK inhibitors also induce autophagy, although for these two compounds the roles of SK1 and SK2 cannot be distinguished.

As a component of its preclinical development, we also tested several combinations of ABC294640 with other anticancer agents in cell culture. We found that two compounds that activate the unfolded protein response, MG-132 and geldanamycin, synergistically elevate the cytotoxicity of ABC294640 in cell culture. These findings are important for the design of anticancer drug combinations for future preclinical and clinical studies and, in particular, suggest a potential use for ABC294640 in the treatment of multiple myeloma. Additional studies suggest efficacy in combination with signaling inhibitors and antimetabolites (unpublished work), making a strong case for broad antitumor activity of ABC294640. The present demonstration of its ability to promote autophagy in tumor cells underscores the need to consider this often-overlooked response in studies of anticancer drugs.

Acknowledgments

We thank Drs. Victoria Findlay and David Turner for help with immunostaining of cells and critical reading of the manuscript; Dr. Venkat Ramshesh from the Cell and Molecular Imaging Core for help with confocal imaging experiments; Rick Peppler for help with flow cytometry experiments; Margaret Romano for preparation of tissue sections; Peng Gao for help with reverse transcription–PCR; and other Smith lab members for useful comments and suggestions.

References

Amaravadi RK, Yu D, Lum JJ, Bui T, Christophorou MA, Evan GI, Thomas-Tikhonenko A, and Thompson CB (2007) Autophagy inhibition enhances therapy-induced apoptosis in a Myc-induced model of lymphoma. *J Clin Invest* **117:**326–336.

Bursch W, Ellinger A, Gerner C, Frohwein U, and Schulte-Hermann R (2000) Programmed cell death (PCD). Apoptosis, autophagic PCD, or others? *Ann NY Acad Sci* **926:**1–12.

Cheng TJ, Wang YJ, Kao WW, Chen RJ, and Ho YS (2007) Protection against arsenic trioxide-induced autophagic cell death in U118 human glioma cells by use of lipoic acid. *Food Chem Toxicol* **45:**1027–1038.

Chou TC and Talalay P (1984) Quantitative analysis of dose–effect relationships: the combined effects of multiple drugs or enzyme inhibitors. *Adv Enzyme Regul* **22:** 27–55.

Cui Q, Tashiro S, Onodera S, Minami M, and Ikejima T (2007) Autophagy preceded apoptosis in oridonin-treated human breast cancer MCF-7 cells. *Biol Pharm Bull* **30:**859–864.

Cuvillier O (2007) Sphingosine kinase-1: a potential therapeutic target in cancer. *Anticancer Drugs* **18:**105–110.

Delgado A, Casas J, Llebaria A, Abad JL, and Fabrias G (2006) Inhibitors of sphingolipid metabolism enzymes. *Biochim Biophys Acta* **1758:**1957–1977.

Ding WX and Yin XM (2008) Sorting, recognition, and activation of the misfolded protein degradation pathways through macroautophagy and the proteasome. *Autophagy* **4:**141–150.

Edwards PA, Tabor D, Kast HR, and Venkateswaran A (2000) Regulation of gene expression by SREBP and SCAP. *Biochim Biophys Acta* **1529:**103–113.
French KJ, Schrecengost RS, Lee BD, Zhuang Y, Smith SN, Eberly JL, Yun JK, and Smith CD (2003) Discovery and evaluation of inhibitors of human sphingosine kinase. *Cancer Res* **63:**5962–5969.
French KJ, Upson JJ, Keller SN, Zhuang Y, Yun JK, and Smith CD (2006) Antitumor activity of sphingosine kinase inhibitors. *J Pharmacol Exp Ther* **318:**596–603.
French KJ, Zhuang Y, Maines LW, Gao P, Wang W, Beljanski V, Upson JJ, Green CL, Keller SN and Smith CD (2010) Pharmacology and antitumor activity of ABC294640, a selective inhibitor of sphingosine kinase-2. *J Pharmacol Exp Ther* doi:10.124/jpet.109.163444.
Fulda S (2009) Tumor resistance to apoptosis. *Int J Cancer* **124:**511–515.
Herman-Antosiewicz A, Johnson DE, and Singh SV (2006) Sulforaphane causes autophagy to inhibit release of cytochrome *C* and apoptosis in human prostate cancer cells. *Cancer Res* **66:**5828–5835.
Hu X and Xuan Y (2008) Bypassing cancer drug resistance by activating multiple death pathways: a proposal from the study of circumventing cancer drug resistance by induction of necroptosis. *Cancer Lett* **259:**127–137.
Igarashi Y, Hakomori S, Toyokuni T, Dean B, Fujita S, Sugimoto M, Ogawa T, el-Ghendy K, and Racker E (1989) Effect of chemically well-defined sphingosine and its *N*-methyl derivatives on protein kinase C and src kinase activities. *Biochemistry* **28:**6796–6800.
Jin S and White E (2008) Tumor suppression by autophagy through the management of metabolic stress. *Autophagy* **4:**563–566.
Klionsky DJ, Abeliovich H, Agostinis P, Agrawal DK, Aliev G, Askew DS, Baba M, Baehrecke EH, Bahr BA, Ballabio A, et al. (2008) Guidelines for the use and interpretation of assays for monitoring autophagy in higher eukaryotes. *Autophagy* **4:**151–175.
Kundu M and Thompson CB (2008) Autophagy: basic principles and relevance to disease. *Annu Rev Pathol* **3:**427–455.
Lavieu G, Scarlatti F, Sala G, Carpentier S, Levade T, Ghidoni R, Botti J, and Codogno P (2006) Regulation of autophagy by sphingosine kinase 1 and its role in cell survival during nutrient starvation. *J Biol Chem* **281:**8518–8527.
Lavieu G, Scarlatti F, Sala G, Carpentier S, Levade T, Ghidoni R, Botti J, and Codogno P (2008) Sphingolipids in macroautophagy. *Methods Mol Biol* **445:**159–173.
Lefranc F, Facchini V, and Kiss R (2007) Proautophagic drugs: a novel means to combat apoptosis-resistant cancers, with a special emphasis on glioblastomas. *Oncologist* **12:**1395–1403.
Maines LW, Fitzpatrick LR, French KJ, Zhuang Y, Xia Z, Keller SN, Upson JJ, and Smith CD (2008) Suppression of ulcerative colitis in mice by orally available inhibitors of sphingosine kinase. *Dig Dis Sci* **53:**997–1012.
Maines LW, French KJ, Wolpert EB, Antonetti DA, and Smith CD (2006) Pharmacologic manipulation of sphingosine kinase in retinal endothelial cells: implications for angiogenic ocular diseases. *Invest Ophthalmol Vis Sci* **47:**5022–5031.
Megidish T, White T, Takio K, Titani K, Igarashi Y, and Hakomori S (1995) The signal modulator protein 14–3-3 is a target of sphingosine- or *N*,*N*-dimethylsphingosine-dependent kinase in 3T3(A31) cells. *Biochem Biophys Res Commun* **216:**739–747.
Meijer AJ and Codogno P (2006) Signaling and autophagy regulation in health, aging, and disease. *Mol Aspects Med* **27:**411–425.
Pattingre S, Bauvy C, Carpentier S, Levade T, Levine B, and Codogno P (2009) Role of JNK1-dependent Bcl-2 phosphorylation in ceramide-induced macroautophagy. *J Biol Chem* **284:**2719–2728.
Poot M, Zhang YZ, Kramer JA, Wells KS, Jones LJ, Hanzel DK, Lugade AG, Singer VL, and Haugland RP (1996) Analysis of mitochondrial morphology and function with novel fixable fluorescent stains. *J Histochem Cytochem* **44:**1363–1372.
Raval J, Lyman S, Nitta T, Mohuczy D, Lemasters JJ, Kim JS, and Behrns KE (2006) Basal reactive oxygen species determine the susceptibility to apoptosis in cirrhotic hepatocytes. *Free Radic Biol Med* **41:**1645–1654.
Ricci MS and Zong WX (2006) Chemotherapeutic approaches for targeting cell death pathways. *Oncologist* **11:**342–357.
Scarlatti F, Bauvy C, Ventruti A, Sala G, Cluzeaud F, Vandewalle A, Ghidoni R, and Codogno P (2004) Ceramide-mediated macroautophagy involves inhibition of protein kinase B and up-regulation of beclin 1. *J Biol Chem* **279:**18384–18391.
Skehan P, Storeng R, Scudiero D, Monks A, McMahon J, Vistica D, Warren JT, Bokesch H, Kenney S, and Boyd MR (1990) New colorimetric cytotoxicity assay for anticancer-drug screening. *J Natl Cancer Inst* **82:**1107–1112.
Smith CD, French KJ, and Zhuang Y (2008) inventors; Apogee Biotechnology Corporation, assignee. Sphingosine kinase inhibitors. U.S. patent 7,338,961. 2008 March 4.
Taha TA, Hannun YA, and Obeid LM (2006) Sphingosine kinase: biochemical and cellular regulation and role in disease. *J Biochem Mol Biol* **39:**113–131.
Taha TA, Osta W, Kozhaya L, Bielawski J, Johnson KR, Gillanders WE, Dbaibo GS, Hannun YA, and Obeid LM (2004) Down-regulation of sphingosine kinase-1 by DNA damage: dependence on proteases and p53. *J Biol Chem* **279:**20546–20554.
Thorburn A (2008) Apoptosis and autophagy: regulatory connections between two supposedly different processes. *Apoptosis* **13:**1–9.
Turcotte S, Chan DA, Sutphin PD, Hay MP, Denny WA, and Giaccia AJ (2008) A molecule targeting VHL-deficient renal cell carcinoma that induces autophagy. *Cancer Cell* **14:**90–102.
Wang M, Tan W, Zhou J, Leow J, Go M, Lee HS, and Casey PJ (2008) A small-molecule inhibitor of isoprenylcysteine carboxymethyltransferase induces autophagic cell death in PC3 prostate cancer cells. *J Biol Chem* **283:**18678–18684.
Wymann MP and Schneiter R (2008) Lipid signaling in disease. *Nat Rev Mol Cell Biol* **9:**162–176.
Yu L, Alva A, Su H, Dutt P, Freundt E, Welsh S, Baehrecke EH, and Lenardo MJ (2004) Regulation of an ATG7-beclin 1 program of autophagic cell death by caspase-8. *Science* **304:**1500–1502.

Address correspondence to: Charles D. Smith, Department of Pharmaceutical and Biomedical Sciences, Medical University of South Carolina, 280 Calhoun Street, MSC140, Charleston, SC 29425. E-mail: smithchd@musc.edu